Surface Electromagnetic Modes of a Ferrite Slab

THOMAS J. GERSON, MEMBER, IEEE, AND JOSEPH S. NADAN, MEMBER, IEEE

Abstract—**The dispersion relationship describing the propagation of electromagnetic (EM) surface modes supported by a ferrite slab of finite thickness magnetized parallel to the planes of its air–ferrite–air or air–ferrite–metal interfaces is investigated. Surface wave propagation at frequencies greater than the ferrite–metal mode resonance is predicted for thick grounded ferrite slabs thereby clarifying prior results based upon semi-infinite and magnetostatic analyses. The relative energy densities of the electromagnetic surface modes is examined at the air–ferrite interfaces of an ungrounded slab.**

INTRODUCTION

THE magnetostatic modes supported by a slab of ferrite material magnetized in the plane of its faces have been investigated by Damon and Eshbach [1]. In this system, surface waves propagate in a direction transverse to the applied static magnetic field in the frequency range $[\omega_i(\omega_i + \omega_m)]^{1/2} < \omega < (\omega_i + \omega_m/2)$, where ω_i is the Larmor precession frequency and ω_m is the magnetization frequency. The dispersion characteristics for wave propagation in the forward and reverse directions are symmetrical about the $k = 0$ axis, the wave amplitude having its maximum at a ferrite–air interface determined by the direction of wave propagation (or the direction of applied static magnetic field). Placing a perfect conducting wall in contact with one of these surfaces destroys this symmetry. However, as demonstrated by Young [2] and Seshadri [3], magnetostatic waves still may propagate in both directions. In addition to the magnetostatic mode of Damon and Eshbach, a magnetostatic ferrite–metal mode is found to propagate in the reverse direction in the frequency range $[\omega_i(\omega_i + \omega_m)]^{1/2} < \omega < (\omega_i + \omega_m)$.

Bresler [4] and Courtois *et al.* [5], have investigated the propagation characteristics of electromagnetic (EM) surface modes at a semi-infinite ferrite–dielectric interface. In addition to a mode closely resembling the magnetostatic surface mode found by Damon and Eshbach, a mode propagating in the opposite direction is supported at the ferrite–dielectric interface. Adopting the nomenclature used in previous investigations of mode spectra supported by longitudinally magnetized ferrite rods [6], the new mode is labeled a dynamic mode since it may only be calculated by including the effects of EM wave propagation, i.e., not making the magnetostatic approximation. The upper frequency limit of this dynamic mode is greater than $(\omega_i + \omega_m)$.

The propagation characteristics of the EM surface waves supported by a ferrite slab of finite thickness with magnetization parallel to its air–ferrite–air interfaces are investigated. By examining the ratio of the surface wave energy densities at the top and bottom surfaces, it is demonstrated that a set of modes resembling the semi-infinite ferrite–dielectric modes is associated with each surface. If a perfect conductor is placed in intimate contact with one of the slab's faces, the modes associated with this surface disappear while those associated with the opposite surface are modified. For thin ferrites the dynamic surface mode is transformed into a mode resembling the magnetostatic ferrite–metal mode. If, however, the slab is sufficiently thick it is found that the grounded slab may support surface wave propagation at frequencies greater than the ferrite–metal mode resonance frequency.

DISPERSION RELATIONSHIP ANALYSIS FOR FINITE FERRITE SLAB

A planar ferrite slab, having magnetization M_0, is bounded by free space as shown in Fig. 1. The slab of thickness d has infinite extent in the $\hat{y}$ and $\hat{z}$ directions. A static magnetic field is applied in the $\hat{z}$ direction, resulting in a uniform field intensity H_i within the ferrite.

EM propagation phenomena are described by Maxwell's equations, which, since both media are insulating, are given by

$$\nabla \times \bar{E} = -\frac{\partial \bar{B}}{\partial t} \tag{1}$$

and

$$\nabla \times \bar{H} = \epsilon \frac{\partial \bar{E}}{\partial t} \tag{2}$$

where ϵ is equal to ϵ_0 in the regions of free space and $\epsilon_m\epsilon_0$ in the ferrite. In the free space regions, $\bar{B}$ and $\bar{H}$ are linearly related by

$$\bar{B} = \mu_0 \bar{H} \tag{3}$$

whereas, in the ferrite, it is assumed that the amplitude of the response of the system to EM excitations is sufficiently small and of the form exp ($j\omega t$) such that $\bar{B}$ and $\bar{H}$ are related by the permeability tensor:

$$||\mu|| = \begin{vmatrix} \mu_{11} & +j\mu_{12} & 0 \\ -j\mu_{12} & \mu_{11} & 0 \\ 0 & 0 & 1 \end{vmatrix} \tag{4}$$

Manuscript received September 28, 1973; revised March 28, 1974. This work was partially supported by the U. S. Air Force Office of Scientific Research (AFSC) under Grant AFSOR-69-1700. This paper represents part of a dissertation submitted by T. J. Gerson to the Department of Electrical Engineering, the City College, City University of New York, N. Y., in partial fulfillment of the requirements for the Ph.D. degree.

T. J. Gerson was with the Department of Electrical Engineering, the City College, City University of New York, N.Y. 10021. He is now with the Department of Electrical Technology, Queensborough Community College, Queens, N.Y.

J. S. Nadan is with the Department of Electrical Engineering, the City College, City University of New York, N.Y. 10021.

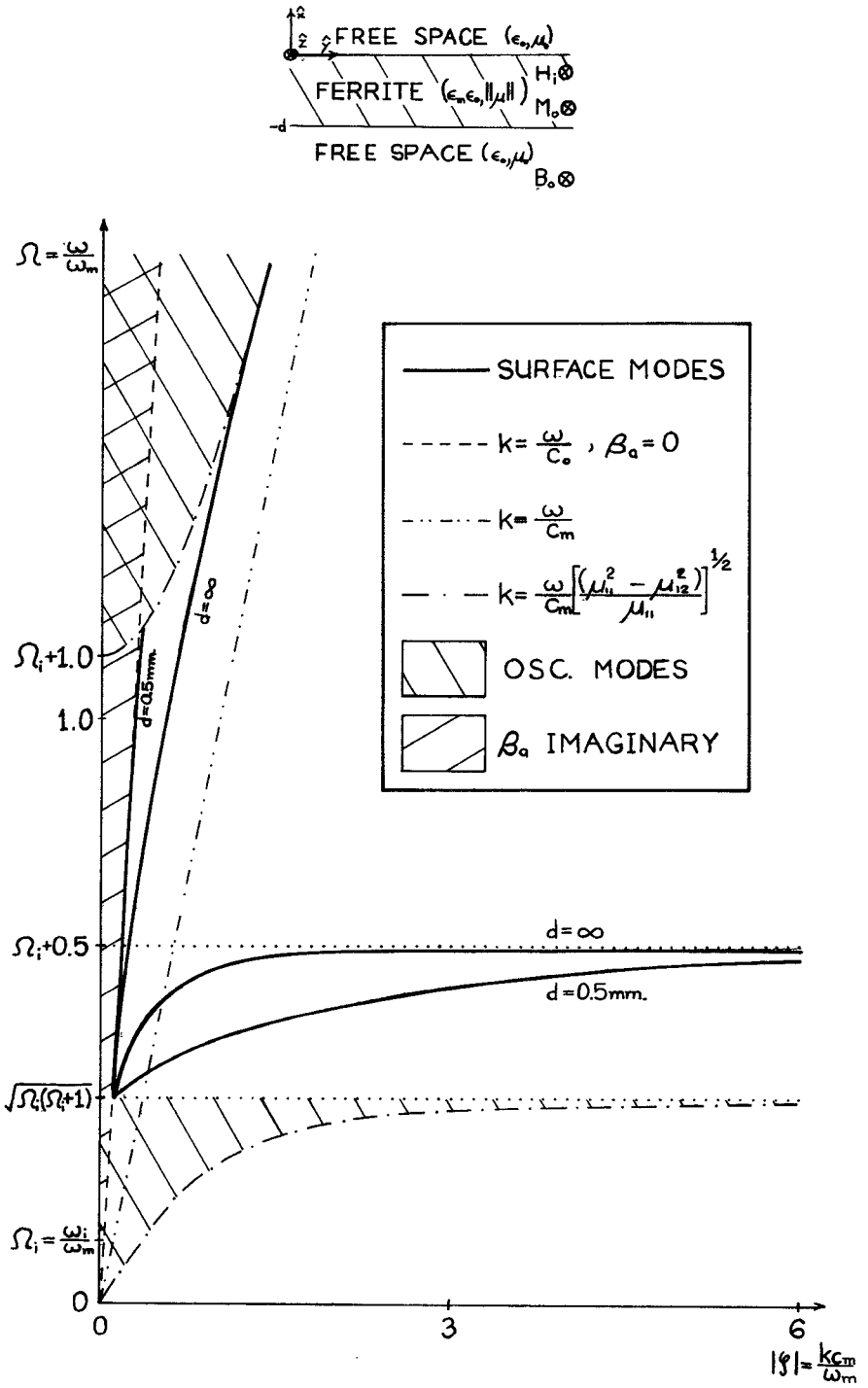

Fig. 1. EM surface wave dispersion for a ferrite slab; $\omega_i/\omega_m = 0.1124$, $\epsilon_m = 14$.

where, neglecting exchange and losses

$$\mu_{11} = 1 + \frac{\omega_i\omega_m}{\omega_i^2 - \omega^2} \tag{5}$$

$$\mu_{12} = \frac{\omega\omega_m}{\omega_i^2 - \omega^2} \tag{6}$$

$$\omega_m = \mu_0\gamma M_0 \tag{7}$$

$$\omega_i = \mu_0\gamma H_i \tag{8}$$

and γ is the gyromagnetic ratio.

The form of the response must be chosen to satisfy Maxwell's equations throughout the media and the boundary conditions at their interfaces while vanishing at infinity. If it is assumed that the system response propagates in the $\hat{y}$ direction, and that $\partial/\partial z = 0$, the form of the electric field may be expressed

$$E_z = A \exp\left[-\beta_a x + j(\omega t - ky)\right], \qquad x > 0 \tag{9}$$

$$E_z = \left[B \cosh \beta_m x + C \sinh \beta_m x\right] \exp\left[j(\omega t - ky)\right], \qquad 0 \geq x \geq -d \tag{10}$$

and

$$E_z = D \exp [\beta_a(x + d) + j(\omega t - ky)], \qquad x < -d \quad (11)$$

where

$$k^2 - \beta_a^2 = \frac{\omega^2}{c_0^2} \quad (12)$$

$$c_0 = \frac{1}{(\epsilon_0\mu_0)^{1/2}} \quad (13)$$

in the free space regions and

$$k^2 - \beta_m^2 = \frac{\omega^2}{c_m^2}\frac{(\mu_{11}^2 - \mu_{12}^2)}{\mu_{11}} \quad (14)$$

$$c_m = \frac{1}{(\epsilon_m\epsilon_0\mu_0)^{1/2}} \quad (15)$$

in the ferrite.

Since the surface current density at the air–ferrite interfaces must be zero, the tangential components of the RF electric and magnetic field intensities must be continuous across these surfaces. Through the application of these boundary conditions and algebraic manipulation the following expressions are obtained:

$$\frac{D}{A} = \cosh \beta_m d - \left[\frac{k\mu_{12} - (\mu_{11}^2 - \mu_{12}^2)\beta_a}{\beta_m\mu_{11}}\right] \sinh \beta_m d \quad (16)$$

and

$$2\mu_{11}\beta_a\beta_m \coth \beta_m d = \frac{k^2\mu_{12}^2 - \beta_m^2\mu_{11}^2 - \beta_a^2(\mu_{11}^2 - \mu_{12}^2)^2}{(\mu_{11}^2 - \mu_{12}^2)}. \quad (17)$$

The first of these equations is an expression relating the amplitude of a mode at the bottom surface with its amplitude on the top surface. The second expression, which appears elsewhere in a similar form [4], is the dispersion equation which relates the transverse wavenumbers of each of the media. Equations (12), (14), and (17) define the mode spectrum supported by the layered structure. It is useful to impose an additional constraint of searching only for solutions of the dispersion relations having real values of β_m, thereby restricting the possible solutions to the nonoscillatory modes whose amplitude varies as a sum of exponentials across the thickness of the ferrite.

In the short wavelength region (large k), where the phase velocity of the response is much smaller than the intrinsic velocity of the ferrite medium,

$$k^2 \cong \beta_m^2 \quad (18)$$

and

$$k^2 \cong \beta_a^2. \quad (19)$$

In this the magnetostatic limit where $\nabla \times \bar{H} \cong 0$ [7], (17) reduces to the result obtained by Damon and Eshbach [1]

$$\omega^2 = \omega_i^2 + \omega_i\omega_m + \frac{\omega_m^2}{2[1 + \coth | k | d]} \quad (20)$$

and plotted by Seshadri [3] for a ferrite with $d = 0.5$ mm, $\epsilon_m = 13$, and $\omega_i/\omega_m = 0.1126$. In this limit the expression for the mode amplitude ratio becomes

$$\frac{D}{A} = \cosh | k | d + \left[\frac{\omega^2 + s\omega\omega_m - (\omega_i + \omega_m)^2}{\omega^2 - \omega_i(\omega_i + \omega_m)}\right] \sinh | k | d \quad (21)$$

where s, defined as [3]

$$s = \frac{k}{| k |} \quad (22)$$

is $+1$ for a forward traveling wave and -1 for a wave traveling in the reverse direction.

The magnetostatic dispersion relationship (20), from which an expression for $| k | d$ may be obtained, predicts that the wavenumber thickness product does not depend on the thickness of the ferrite. Hence, from (18), $\beta_m d$ does not vary as d is increased. One may therefore conclude that although the wavelength of the response is affected by varying the ferrite thickness, the relative surface wave amplitudes are unaffected, a limit inherent to the magnetostatic approximation.

For the thick ferrite case, $\beta_m \coth \beta_m d \cong | \beta_m |$, (17), which includes EM propagation effects reduces to [3]

$$[(\mu_{11}^2 - \mu_{12}^2)\beta_a - k\mu_{12} + \beta_m\mu_{11}] \cdot [(\mu_{11}^2 - \mu_{12}^2)\beta_a + k\mu_{12} + \beta_m\mu_{11}] = 0. \quad (23)$$

The mode set represented by the terms in the left bracket corresponds to surface modes for the semi-infinite model where the ferrite occupies the lower half-space; whereas the mode set represented by the terms in the right bracket describes surface wave propagation for the semi-infinite model where the ferrite occuipes the upper half-space. This second set of modes differs from the first only in that the modes propagate in opposite directions. It is noted that the directions of propagation for the modes found by Courtois *et al.* [5], are reversed due to an error in the sign of the off-diagonal permeability tensor components as shown by Bolle and Lewin [8].

Thus in the thick film limit the ferrite slab may support four surface modes, two "dynamic" modes, and two modes, which because of their resemblance to the magnetostatic modes of Damon and Eshbach are termed "magnetostatic." Of the modes associated with the top surface, the forward mode is "magnetostatic" and is labeled $s = +1_m$, while the reverse mode, termed $s = -1_d$, is "dynamic." Similarly, the modes associated with the bottom face are a forward "dynamic" mode, $s = +1_d$, and a reverse "magnetostatic" mode, $s = -1_m$.

To determine the effects of ferrite thickness (12), (14), (16), and (17) must be solved numerically. This

process may be simplified by noting that the dispersion relationships are symmetrical in k and β_m. Since the mode amplitude relations are also symmetrical in β_m only positive β_m need be considered. The dispersion relationships are solved using standard numerical techniques and are plotted in Fig. 1 for $\epsilon_m = 14$, $\omega_i/\omega_m = 0.1124$, and a ferrite thickness of 0.5 mm. (The semi-infinite ferrite case is included in the diagram for comparison.) With the exception of the lower frequency limit where $k = \omega/c_0$, the magnitude of the wavenumbers of the "dynamic" modes is reduced for any given frequency by decreasing the thickness of the ferrite film. For $d = 0.5$ mm, the magnitude of the phase velocities of the dynamic modes is only slightly less than the intrinsic velocity in the free space regions. The "magnetostatic" modes which are strongly dependent on the spin system suffer a decrease in wavelength over most of their spectrum due to the finite geometry. As either the lower cutoff or resonance frequency is approached, the transverse wavenumber β_m increases, with the result that the mode is less dependent on the thickness of the ferrite and approaches the infinite ferrite results.

The ratio of the surface wave energy densities at the top and bottom surfaces is plotted in Fig. 2 for the "dynamic" and "magnetostatic" modes of Fig. 1. In agreement with the thick ferrite results, the forward "dynamic" and reverse "magnetostatic" mode amplitudes are larger at the top surface than at the bottom surface, while the opposite is true for the two other modes. Thus if conditions existing at the bottom face of the ferrite are modified, it is expected that the modes associated with the bottom surface would be more strongly affected than those associated with the top face. The modification of the environment on one side of the ferrite not only alters the relative amplitudes of the modes at the two surfaces, but also has the effect of destroying the symmetry of propagation characteristics at the upper and lower ferrite surfaces [9]. An extreme example of this occurs when the RF electric field at the bottom surface is set to zero by placing this surface in intimate contact with a perfect conductor [2]–[4], [10].

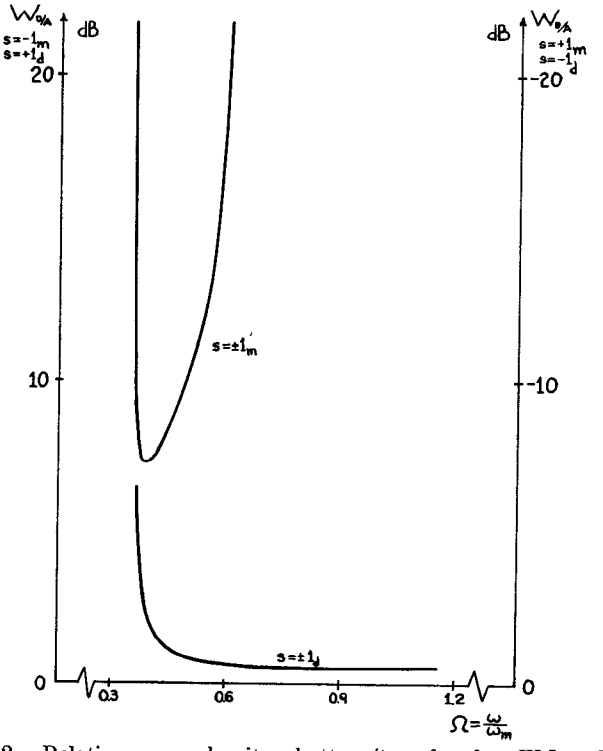

Fig. 2. Relative energy density—bottom/top of surface EM modes of a ferrite slab; $d = 0.5$ mm, $\omega_i/\omega_m = 0.1124$, $\epsilon_m = 14$.

DISPERSION RELATIONSHIP ANALYSIS FOR GROUNDED FERRITE SLAB

The analysis of the ferrite slab terminated in a ground plane at $x = -d$ proceeds in a similar manner to that performed above, with the exception of new boundary conditions at the $x = -d$ interface. The requirement that the RF electric field in the plane of the interface must be zero at the ferrite–metal boundary leads to a condition relating the coefficients of the fields in the air and ferrite regions:

$$A = B = C \tanh \beta_m d. \tag{24}$$

Satisfying the boundary condition on the RF magnetic field intensity at the ferrite–air interface results in the dispersion equation relating the transverse wavenumbers of both media [4], [11]:

$$\beta_a = \frac{k\mu_{12} - \beta_m \mu_{11} \coth \beta_m d}{(\mu_{11}^2 - \mu_{12}^2)}. \tag{25}$$

For the thick ferrite case, the metal is far removed from the air–ferrite interface; in the limit as $d \to \infty$, (25) reduces to the dispersion relation for the semi-infinite model as anticipated. In the magnetostatic limit (25) reduces to the results obtained by Young [2] for $n = 0$ and Seshadri [3] for a ferrite slab grounded by a perfect conductor. (The lossy conductor case has been studied in the magnetostatic limit by De Wames and Wolfram [12].) The lossless magnetostatic model predicts that the ferrite–metal ($s = -1$) mode has a resonance at $\omega = \omega_i + \omega_m$ for all ferrite thicknesses. However, since the model predicts that the magnitude of the surface mode wavenumber at any given frequency must decrease as the ferrite thickness increases, the portion of the spectrum over which EM wave propagation may be neglected is reduced as the ferrite thickness is increased. The magnetostatic model also predicts that the upper frequency limit for surface wave propagation on grounded ferrites is $\omega = \omega_i + \omega_m$, whereas EM analysis of the semi-infinite case has shown that surface waves may propagate above this limit. To determine whether such modes exist for finite grounded ferrites, the dispersion relation must be solved numerically.

The surface wave dispersion relationship is plotted in Fig. 3 with ferrite thickness as a parameter. Considering first the portion of the spectrum below the ferrite mode

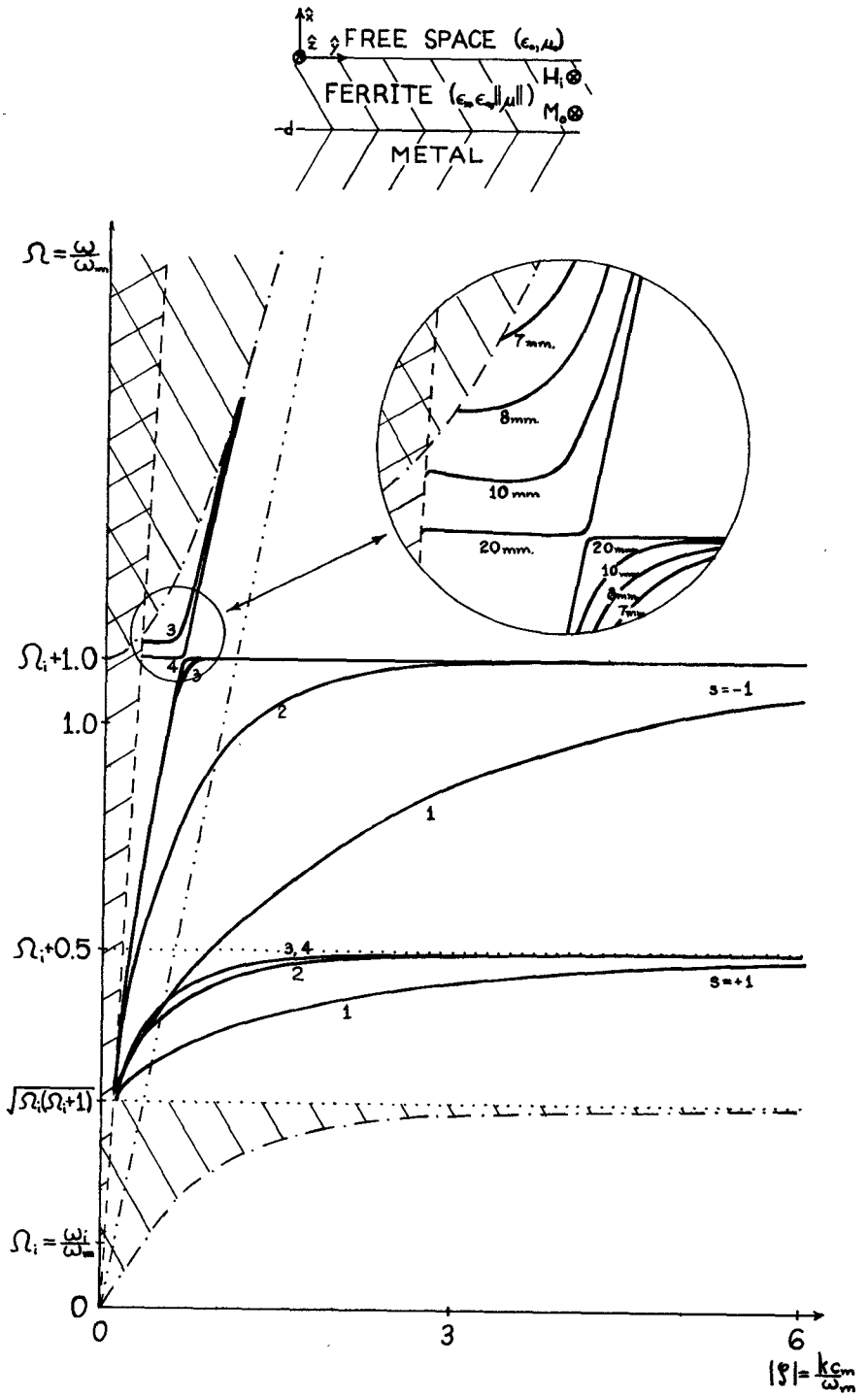

Fig. 3. Surface EM modes of a grounded ferrite slab; 1—d = 0.5 mm; 2—d = 2 mm; 3—d = 10 mm; 4—d = 20 mm; $\omega_i/\omega_m = 0.1124$, $\epsilon_m = 14$.

resonance it is observed that, with the exception of the long wavelength region, the dispersion curve for a 0.5-mm ferrite thickness is similar to that found using the magnetostatic approximation. As the thickness of the ferrite is increased, the wavenumber at any given frequency decreases, and the dispersion characteristic approaches the characteristics obtained for the thick or semi-infinite case, the $d = \infty$ curve in Fig. 1, except that the resonance predicted by using the magnetostatic approximation is retained for all finite values of ferrite thickness. Thus, while the semi-infinite model may be appropriate near the lower end of the $s = -1$ mode spectrum, it is not appropriate near the ferrite–metal mode resonance, even for relatively thick ferrites. The metamorphosis in the character of the mode is made apparent by considering the variation of the amplitudes of the RF magnetic field components across the sample, as shown in Fig. 4 for a 10-mm thickness. The curves,

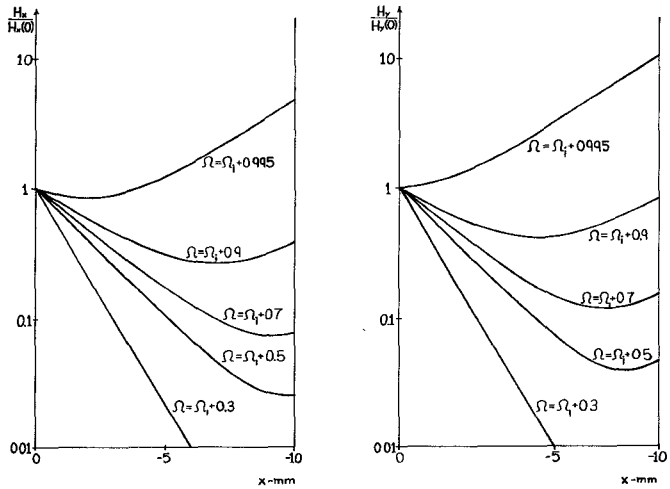

Fig. 4. Variation of normalized magnetic field intensity components across the thickness of a 10-mm grounded ferrite slab; $\omega_s/\omega_m = 0.1124$, $\epsilon_m = 14$.

normalized with respect to the amplitudes attained at the ferrite-free-space interface, show that near the lower end of the $s = -1$ mode spectrum, the magnetic field intensity magnitudes are greatest at the free-space boundary and decrease rapidly towards the interior of the ferrite. In this region of the spectrum the field configuration of the mode closely resembles that of the dynamic mode in the semi-infinite case. As the frequency is increased a transition takes place in which the points where the magnetic field intensity components attain minima shift towards the ferrite-free-space interface. For frequencies just below the magnetostatic $s = -1$ mode resonance ($\Omega = \Omega_i + 1.0$) the wave takes on the appearance of a ferrite–metal mode, the magnitudes of the magnetic field intensity components having maxima at the metallic boundary and decreasing monotonically as the free space boundary is approached. It is noted that as the ferrite becomes increasingly thick, the transition to ferrite–metal mode behavior takes place closer to the resonant frequency, the resonance becoming increasingly sharp and thus subject to the deletive effects of ferrite losses.

Immediately above the $s = -1$ mode resonance frequency, there is a range, shown in greater detail in the Fig. 3 insert, for which a surface wave solution does not exist. If the ferrite is sufficiently thick, this cutoff region is of limited extent, the ferrite grounded by a perfect conductor supporting surface waves at frequencies greater than the ferrite–metal mode resonance, as illustrated by the upper branches of the 10-mm and 20-mm curves in Fig. 3. These characteristics are observed to originate at the $\beta_a = 0$ curve and approach the semi-infinite dynamic mode solution as the wavenumber increases. However, the upper frequency limits (where the surface wave characteristic merges with the $\beta_m = 0$ curve) are lower than predicted by the semi-infinite model. As these upper frequency limits are approached β_m becomes small signifying that the fields vary only slightly across the sample's thickness. At the cutoff ($\beta_m = 0$) the RF electric field is zero throughout the ferrite, the conductor, in effect, "shorting out" the surface wave at the opposite surface.

As the thickness of the grounded ferrite decreases, the passband of the upper branch $s = -1$ surface mode decreases. As indicated by the 7- and 8-mm curves, the mode originates at the $\beta_m = 0$ curve (not at the $\beta_a = 0$ curve) where it couples to the oscillatory modes in the bulk. As the ferrite thickness is further reduced, the upper and lower frequency limits approach one another until, at approximately 6.38 mm, they merge, resulting in the disappearance of this portion of the spectrum. On the other hand, it is observed that as the ferrite thickness increases, the range for which the $s = -1$ mode is cutoff decreases. In the semi-infinite limit, the upper and lower branches of the $s = -1$ mode spectrum coalesce with the result that both the cutoff and the resonance are eliminated.

CONCLUSIONS

Dispersion relationships describing EM surface wave propagation on finite thickness ferrite slabs have been analyzed extending previous results based on the magnetostatic and semi-infinite models and providing an improved understanding of the relative magnitudes of the surface modes at the top and bottom faces. The magnetostatic ferrite–metal mode has been shown to be closely related to the "dynamic" mode of the semi-infinite model, one transforming to the other as the thickness of the grounded ferrite slab is varied. When the grounded ferrite is sufficiently thick, surface waves propagate at frequencies greater than the ferrite–metal mode resonance frequency, previously thought to be the upper frequency limit.

REFERENCES

[1] R. W. Damon and J. R. Eshbach, "Magnetostatic modes of a ferromagnetic slab," *J. Phys. Chem. Solids*, vol. 19, pp. 308–320, 1961.

[2] a) P. Young, "Efficient broadband excitation of the $n = 0$ surface magnetostatic waves in a Y.I.G. slab," *Electron. Lett.*, vol. 4, pp. 566–568, 1968.
b) ——, "Effect of boundary conditions on the propagation of surface magnetostatic waves in a transversely magnetized thin Y.I.G. slab," *Electron. Lett.*, vol. 5, pp. 429–431, 1969.

[3] S. R. Seshadri, "Surface magnetostatic modes of a ferrite slab," *Proc. IEEE* (Lett.), vol. 58, pp. 506–507, Mar. 1970.

[4] A. D. Bresler, "TE_{no} surface waves at ferrite-air interfaces," Polytech. Inst. Brooklyn, Microwave Res. Inst., Memo 48, R-723-59, PIB-651, 1959.

[5] L. Courtois, G. Declercq, and M. Peurichard, "On the nonreciprocal aspect of gyromagnetic surface waves," in *AIP Conf. Proc.*, pt. 2, 1970, pp. 1541–1545.

[6] a) F. W. Schott, T. F. Tao, and R. A. Freibrun, "Electromagnetic waves in longitudinally magnetized ferrite rods," *J. Appl. Phys.*, vol. 38, pp. 3015–3022, 1967.
b) F. W. Schott and T. F. Tao, "On the classification of electromagnetic waves in ferrite rods," *IEEE Trans. Microwave Theory Tech.* (Corresp.), vol. MTT-16, pp. 959–961, Nov. 1968.

[7] L. R. Walker, "Magnetostatic modes in ferromagnetic resonance," *Phys. Rev.*, vol. 105, pp. 390–399, 1957.

[8] D. M. Bolle and L. Lewin, "On the definition of parameters in ferrite–electromagnetic wave interactions," *IEEE Trans. Microwave Theory Tech.*, vol. MTT-21, p. 118, Feb. 1973.

[9] a) M. L. Kales, H. N. Chait, and N. G. Sokiotis, "A nonreciprocal microwave component," *J. Appl. Phys. Lett.*, vol. 24, pp. 816–817, 1953.
b) B. Lax, K. J. Button, and L. M. Roth, "Ferrite phase shifters in rectangular wave guide," *J. Appl. Phys.*, vol. 25, pp. 1413–1421, 1954.
c) H. Seidel, "Ferrite slabs in transverse electronic mode wave guide," *J. Appl. Phys.*, vol. 28, pp. 218–226, 1957.
d) H. Seidel and R. C. Fletcher, "Gyromagnetic modes in wave-

guide partially loaded with ferrite," *Bell Syst. Tech. J.*, vol. 38, pp. 1427–1456, 1959.
e) W. L. Bongianni, "Magnetostatic propagation in a dielectric layered structure," *J. Appl. Phys.*, vol. 43, pp. 2541–2548, 1972.
f) D. F. Vaslow, "Group delay time for the surface wave on a YIG film backed by a grounded dielectric slab," *Proc. IEEE* (Lett.), vol. 61, pp. 142–143, Jan. 1973.
[10] a) L. K. Brundle and N. J. Freedman, "Magnetostatic surface waves on a Y. I. G. slab," *Electron. Lett.*, vol. 4, pp. 132–134, 1968.
b) R. Pauchard, B. Désormière, and J. Guidevaux, "Electromagnetic surface waves in a metallised ferrite slab," *Electron. Lett.*, vol. 7, pp. 428–430, 1971.
[11] a) B. Lax and K. J. Button, "Theory of new ferrite modes in rectangular wave guide," *J. Appl. Phys. Lett.*, vol. 26, pp. 1184–1185, 1955.
b) K. J. Button and B. Lax, "Theory of ferrites in rectangular waveguides," *IRE Trans. Antennas Propagat.*, vol. AP-4, pp. 531–537, July 1956.
[12] R. E. De Wames and T. Wolfram, "Characteristics of magnetostatic surface waves for a metalized ferrite slab," *J. Appl. Phys.*, vol. 41, pp. 5243–5246, 1970.

A New Interdigital Electrode Transducer Geometry

KENNETH M. LAKIN, MEMBER, IEEE, DAVID W. T. MIH, AND ROBERT M. TARR

***Abstract*—A new interdigital electrode transducer geometry has been conceived and its theoretical performance verified experimentally. The transducer is composed of sets of electrodes which are connected in series through an offset or "dog-leg" electrode, thereby significantly increasing the electrical impedance of the transducer over that of a conventional one having the same aperture. This transducer radiates and receives a uniform straight-crested wavefront. The transducer is shown to have unique impedance properties suited for wide-aperture surface-wave devices or those requiring some form of wave-amplitude weighting.**

Experiments have been conducted on *YZ* $LiNbO_3$ which verify that the terminal impedance of the transducer is proportional to the square of the number of equal-aperture constant-amplitude sections.

I. INTRODUCTION

INTERDIGITAL electrode transducers (IDT), employed for surface acoustic-wave generation, have a fundamental property that the terminal electrical impedance is inversely proportional to the width of the electrode overlap or beam aperture [1]. This property is exhibited if the electrode voltage is independent of aperture since then the displacement current is proportional to electrode area and, hence, width. A given transducer's width is chosen as a compromise between a number of factors which are: a) electrode conduction loss, b) capacitance and implied relative ease of tuning, c) resultant radiation resistance compared to source and load impedances which affects mismatch loss and surface-wave reflection (regeneration), d) diffraction effects due to propagation distance in relation to chosen width, and e) in some cases, available substrate size. Factor d) may be reduced by using wider apertures, which lower the electrical impedance, or diffraction loss may be compensated for by use of aperture weighting if the effects are accurately predictable. Narrow apertures may, however, be required in pulse-compression filter transducers [2] where a large array will have, at any one frequency, an active section in shunt with the large capacitance of the inactive region. The large shunt capacitance has the effect of transforming active section impedances to much lower values which can only be partially offset in magnitude by a small aperture design. Frequency or phase filter synthesis requires aperture weighting such that small electrode overlap regions have higher impedance and draw less current, hence radiate less power, than wider aperture regions. The classic rectangular passband frequency filter, for example, requires a sin x/x weighting in the transducer spatial domain where the spatial sidelobes of the sin x/x aperture distribution ultimately determine the frequency passband amplitude response. However, in a given fabrication, the spatial sidelobe overlap distribution may result in apertures of only a few wavelengths and, because of diffraction effects, the effective weighting of these spatial sidelobes is difficult to determine.

The point of the preceding discussion is to indicate the desirability of a transducer geometry which offers some flexibility in the relation between impedance and aperture. A desirable transducer might be composed of electrodes which radiate identical, or nearly identical, width waves yet having each electrode's efficiency determined by a parameter other than overlap aperture. This paper describes one approach, illustrated in Fig. 1, which employs interdigital electrode arrays arranged in a unique manner that results in a more flexible impedance versus aperture relationship, and radiates uniform plane waves from electrode pairs having the usual half-wavelength periodicity in the direction of propagation. A uniform straight-

Manuscript received December 6, 1973; revised April 8, 1974. This work was supported in part by the Air Force Office of Scientific Research under Contract AFOSR-72-2391, in part by the Joint Services Electronics Program through the Air Force Office of Scientific Research/AFSC under Contract F44620-71-C-0067, and in part by the Office of Naval Research under Contract N00014-67-0269-0018.

The authors are with the Electronic Sciences Laboratory, University of Southern California, Los Angeles, Calif. 90007.